

Gut Microbiota from Twins Discordant for Obesity Modulate Metabolism in Mice

Vanessa K. Ridaura, Jeremiah J. Faith, Federico E. Rey, Jiye Cheng, Alexis E. Duncan, Andrew L. Kau, Nicholas W. Griffin, Vincent Lombard, Bernard Henrissat, James R. Bain, Michael J. Muehlbauer, Olga Ilkayeva, Clay F. Semenkovich, Katsuhiko Funai, David K. Hayashi, Barbara J. Lyle, Margaret C. Martini, Luke K. Ursell, Jose C. Clemente, William Van Treuren, William A. Walters, Rob Knight, Christopher B. Newgard, Andrew C. Heath, Jeffrey I. Gordon*

Introduction: Establishing whether specific structural and functional configurations of a human gut microbiota are causally related to a given physiologic or disease phenotype is challenging. Twins discordant for obesity provide an opportunity to examine interrelations between obesity and its associated metabolic disorders, diet, and the gut microbiota. Transplanting the intact uncultured or cultured human fecal microbiota from each member of a discordant twin pair into separate groups of recipient germ-free mice permits the donors' communities to be replicated, differences between their properties to be identified, the impact of these differences on body composition and metabolic phenotypes to be discerned, and the effects of diet-by-microbiota interactions to be analyzed. In addition, cohousing coprophagic mice harboring transplanted microbiota from discordant pairs provides an opportunity to determine which bacterial taxa invade the gut communities of cage mates, how invasion correlates with host phenotypes, and how invasion and microbial niche are affected by human diets.

Methods: Separate groups of germ-free mice were colonized with uncultured fecal microbiota from each member of four twin pairs discordant for obesity, or with culture collections from an obese (Ob) or lean (Ln) co-twin. Animals were fed a mouse chow low in fat and rich in plant polysaccharides (LF-HPP) or one of two diets reflecting the upper or lower (Hi or Lo) tertiles of consumption of saturated fats (SF) and fruits and vegetables (FV) based on the U.S. National Health and Nutrition Examination Survey (NHANES). Ln or Ob mice were cohoused 5 days after colonization. Body composition changes were defined by quantitative magnetic resonance. Microbiota or microbiome structure, gene expression, and metabolism were assayed by 16S ribosomal RNA profiling, whole-community shotgun sequencing, RNA-sequencing, and mass spectrometry. Host gene expression and metabolism were also characterized.

Results and Discussion: The intact uncultured and culturable bacterial component of Ob co-twins' fecal microbiota conveyed significantly greater increases in body mass and adiposity than those of Ln communities. Differences in body composition were correlated with differences in fermentation of short-chain fatty acids (increased in Ln), metabolism of branched-chain amino acids (increased in Ob), and microbial transformation of bile acid species (increased in Ln and correlated with down-regulation of host farnesoid X receptor signaling). Cohousing Ln and Ob mice prevented development of increased adiposity and body mass in Ob cage mates and transformed their microbiota's metabolic profile to a leanlike state. Transformation correlated with invasion of members of Bacteroidales from Ln into Ob microbiota. Invasion and phenotypic rescue were diet-dependent and occurred with the diet representing the lower tertile of U.S. consumption of saturated fats and upper tertile of fruits and vegetables but not with the diet representing the upper tertile of saturated fats and lower tertile of fruit and vegetable consumption. These results reveal that transmissible and modifiable interactions between diet and microbiota influence host biology.

READ THE FULL ARTICLE ONLINE

<http://dx.doi.org/10.1126/science.1241214>



Cite this article as V. K. Ridaura *et al.*, *Science* **341**, 1241214 (2013). DOI: 10.1126/science.1241214

FIGURES IN THE FULL ARTICLE

Fig. 1. Reliable replication of human donor microbiota in gnotobiotic mice.

Fig. 2. Cohousing Ob^{ch} and Ln^{ch} mice transforms the adiposity phenotype of cage mates harboring the obese co-twin's culture collection to a leanlike state.

Fig. 3. Effect of cohousing on metabolic profiles in mice consuming the LF-HPP diet.

Fig. 4. Effects of NHANES-based LoSF-HiFV and HiSF-LoFV diets on bacterial invasion, body mass, and metabolic phenotypes.

Fig. 5. Invasion analysis of species-level taxa in Ob^{ch} or Ln^{ch} mice fed the NHANES-based LoSF-HiFV diet.

Fig. 6. Acylcarnitine profile in the skeletal muscle of mice colonized with the Ob or Ln culture collections from dizygotic twin pair 1 and fed the LoSF-HiFV diet.

SUPPLEMENTARY MATERIALS

Materials and Methods

Supplementary Text

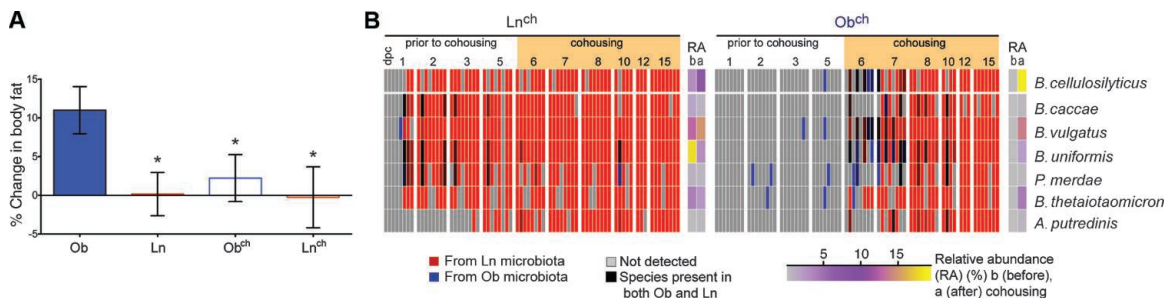
Figs. S1 to S17

Tables S1 to S17

References and Notes

RELATED ITEMS IN SCIENCE

A. W. Walker, J. Parkhill, Fighting obesity with bacteria. *Science* **341**, 1069–1070 (2013). DOI: 10.1126/science.1243787



Cohousing Ln and Ob mice prevents adiposity phenotype in Ob cage mates (Ob^{ch}). (A) The adiposity change after 10 days of cohousing. **P* < 0.05 versus Ob controls (Student's *t* test). (B) Bacteroidales from Ln^{ch} microbiota invade the Ob^{ch} microbiota. Columns show individual mice.

The list of author affiliations is available in the full article online.

*Corresponding author. E-mail: jgordon@wustl.edu

Gut Microbiota from Twins Discordant for Obesity Modulate Metabolism in Mice

Vanessa K. Ridaura,¹ Jeremiah J. Faith,¹ Federico E. Rey,¹ Jiye Cheng,¹ Alexis E. Duncan,^{2,3} Andrew L. Kau,¹ Nicholas W. Griffin,¹ Vincent Lombard,⁴ Bernard Henrissat,^{4,5} James R. Bain,^{6,7,8} Michael J. Muehlbauer,⁶ Olga Ilkayeva,⁶ Clay F. Semenkovich,⁹ Katsuhiko Funai,⁹ David K. Hayashi,¹⁰ Barbara J. Lyle,¹¹ Margaret C. Martini,¹¹ Luke K. Ursell,¹² Jose C. Clemente,¹² William Van Treuren,¹² William A. Walters,¹³ Rob Knight,^{12,14,15} Christopher B. Newgard,^{6,7,8} Andrew C. Heath,² Jeffrey I. Gordon^{1*}

The role of specific gut microbes in shaping body composition remains unclear. We transplanted fecal microbiota from adult female twin pairs discordant for obesity into germ-free mice fed low-fat mouse chow, as well as diets representing different levels of saturated fat and fruit and vegetable consumption typical of the U.S. diet. Increased total body and fat mass, as well as obesity-associated metabolic phenotypes, were transmissible with uncultured fecal communities and with their corresponding fecal bacterial culture collections. Cohousing mice harboring an obese twin's microbiota (Ob) with mice containing the lean co-twin's microbiota (Ln) prevented the development of increased body mass and obesity-associated metabolic phenotypes in Ob cage mates. Rescue correlated with invasion of specific members of Bacteroidetes from the Ln microbiota into Ob microbiota and was diet-dependent. These findings reveal transmissible, rapid, and modifiable effects of diet-by-microbiota interactions.

Microbial community configurations vary substantially between unrelated individuals (1–9), which creates a challenge in designing surveys of sufficient power to determine whether observed differences between disease-associated and healthy communities differ significantly from normal interpersonal variation. This challenge is especially great if, for a given disease state, there are many associated states of the microbial species (microbiota) or microbial gene repertoire (microbiome), each shared by relatively few individuals. Microbiota config-

urations are influenced by early environmental exposures and are generally more similar among family members (2, 7, 10, 11).

There have been conflicting reports about the relation between interpersonal differences in the structure of the gut microbiota and host body mass index (BMI). Taxonomic profiles for obese and lean individuals may have distinct patterns between human populations, but technical issues related to how gut samples are processed and community members are identified by 16S ribosomal RNA (rRNA) gene sequencing may also play a role in observed differences. The relative contributions of the microbiota and dietary components to obesity and obesity-related metabolic phenotypes are unclear and likely multifaceted (2, 12–17). Transplants of fecal microbiota from healthy donors to recipients with metabolic syndrome have provided evidence that the microbiota can ameliorate insulin-resistance, although the underlying mechanisms remain unclear (18).

Monozygotic (MZ) or dizygotic (DZ) twins discordant for obesity (19, 20) provide an attractive model for studying the interrelations between obesity, its associated dietary and lifestyle risk factors, and the gut microbiota/microbiome. In the case of same-sex twins discordant for a disease phenotype, the healthy co-twin provides a valuable reference control to contrast with the co-twin's disease-associated gut community. However, this comparison is fundamentally descriptive and cannot establish causality. Transplanting a fecal sample obtained from each twin in a discordant pair into separate groups of recipient germ-free mice provides an opportunity to (i) identify structural and functional

differences between their gut communities; (ii) generate and test hypotheses about the impact of these differences on host biology, including body composition and metabolism; and (iii) determine the effects of diet-by-microbiota interactions through manipulation of the diets fed to these “humanized” animals and/or the representation of microbial taxa in their gut communities.

Reproducibility of Microbiota Transplants from Discordant Twins

We surveyed data collected from 21- to 32-year-old female twin pairs ($n = 1539$) enrolled in the Missouri Adolescent Female Twin Study [MOAFTS; (21, 22); for further details, see ref. (23)]. We recruited four twin pairs, discordant for obesity (obese twin BMI > 30 kg/m²) with a sustained multiyear BMI difference of ≥ 5.5 kg/m² ($n = 1$ MZ and 3 DZ pairs) (Fig. 1A). Fecal samples were collected from each twin, frozen immediately after they were produced, and stored at -80°C . Each fecal sample was introduced, via a single oral gavage, into a group of 8- to 9-week-old adult male germ-free C57BL/6J mice (one gnotobiotic isolator per microbiota sample; each recipient mouse was individually caged within the isolator; $n = 3$ to 4 mice per donor microbiota sample per experiment; $n = 1$ to 5 independent experiments per microbiota). All recipient mice were fed, ad libitum, a commercial, sterilized mouse chow that was low in fat (4% by weight) and high in plant polysaccharides (LF-HPP) (23). Fecal pellets were obtained from each mouse 1, 3, 7, 10, and 15 days post colonization (dpc) and, for more prolonged experiments, on days 17, 22, 24, 29, and 35.

Unweighted UniFrac-based comparisons of bacterial 16S rRNA data sets generated from the input human donor microbiota, from fecal samples collected from gnotobiotic mice and from different locations along the length of the mouse gut at the time they were killed (table S1A), plus comparisons of the representation of genes with assignable enzyme commission numbers (ECs) in human fecal and mouse cecal microbiomes (defined by shotgun sequencing), disclosed that transplant recipients efficiently and reproducibly captured the taxonomic features of their human donor's microbiota and the functions encoded by the donor's microbiome (see Fig. 1B; fig. S1, A to E; fig. S2; table S1B; and table S2, A to D) (23). The 16S rRNA data sets allowed us to identify bacterial taxa that differentiate gnotobiotic mice harboring gut communities transplanted from all lean versus all obese co-twins [analysis of variance (ANOVA) using Benjamini-Hochberg correction for multiple hypotheses] [table S3; see (23) for details].

Reproducible Transmission of Donor Body Composition Phenotypes

Quantitative magnetic resonance (QMR) analysis was used to assess the body composition of transplant recipients 1 day, 15 days, and, in

¹Center for Genome Sciences and Systems Biology, Washington University School of Medicine, St. Louis, MO 63108, USA. ²Department of Psychiatry, Washington University School of Medicine, St. Louis, MO 63110, USA. ³George Warren Brown School of Social Work, Washington University, St. Louis, MO 63130, USA. ⁴Architecture et Fonction des Macromolécules Biologiques, CNRS and Aix Marseille Université, CNRS UMR 7257, 13288 Marseille, France. ⁵Department of Cellular and Molecular Medicine, Faculty of Health and Medical Sciences, University of Copenhagen, DK-2200, Copenhagen, Denmark. ⁶Sarah W. Stedman Nutrition and Metabolism Center, Duke University Medical Center, Durham, NC 27710, USA. ⁷Department of Medicine, Duke University Medical Center, Durham, NC 27710, USA. ⁸Department of Pharmacology and Cancer Biology, Duke University Medical Center, Durham, NC 27710, USA. ⁹Department of Medicine, Washington University School of Medicine, St. Louis, MO 63110, USA. ¹⁰Mondelez International, Glenview, IL 60025, USA. ¹¹Kraft Foods Group, Glenview, IL 60025, USA. ¹²Department of Chemistry and Biochemistry, University of Colorado, Boulder, CO 80309, USA. ¹³Molecular, Cellular and Developmental Biology, University of Colorado, Boulder, CO 80309, USA. ¹⁴BioFrontiers Institute, University of Colorado, Boulder, CO 80309, USA. ¹⁵Howard Hughes Medical Institute, University of Colorado, Boulder, CO 80309, USA.

*To whom correspondence should be sent. E-mail: jgordon@wustl.edu

the case of longer experiments, 8, 22, 29, and 35 days after transplantation. The increased adiposity phenotype of each obese twin in a discordant twin pair was transmissible: The change in adipose mass of mice that received an obese co-twin's fecal microbiota was significantly greater than the change in animals receiving her lean twin's gut community within a given experiment and was reproducible across experiments ($P \leq 0.001$, one-tailed unpaired Student's t test; $n = 103$ mice phenotyped) (Fig. 1, C to E). Epididymal fat pad weights (normalized to total body weight) were also significantly higher in mice colonized with gut communities from obese twins ($P \leq 0.05$, one-tailed unpaired Student's t test). These differences in adiposity were not associated with statistically significant differences in daily chow consumption (measured on days 1, 8, and 15 after gavage and weekly thereafter for longer experiments) or with appreciably greater inflammatory responses in recipients of obese compared with lean co-twin fecal microbiota as judged by fluorescence-activated cell sorting (FACS) analysis of the CD4⁺ and CD8⁺ T cell compartments in spleen, mesenteric lymph nodes, small intestine, or colon [see (23) for details].

Functional Differences Between Transplanted Microbial Communities

Fecal samples collected from gnotobiotic mice were used to prepare RNA for microbial RNA sequencing (RNA-Seq) of the transplanted microbial communities' meta-transcriptomes (table S1C). Transcripts were mapped to a database of sequenced human gut bacterial genomes and assigned to *Kyoto Encyclopedia of Genes and Genomes* (KEGG) Enzyme Commission numbers (EC numbers) [see ref. (23)]. Significant differences and distinguishing characteristics were defined using ShotgunFunctionalizeR, which is based on a Poisson model (24) (see table S4 and table S5 for ECs and KEGG level 2 pathways, respectively). Transcripts encoding 305 KEGG ECs were differentially expressed between mice harboring microbiomes transplanted from lean or obese donors [ShotgunFunctionalizeR, Akaike's information criterion (AIC) < 5000; $P \leq 10^{-30}$].

Mice harboring the transplanted microbiomes from the obese twins exhibited higher expression of microbial genes involved in detoxification and stress responses; in biosynthesis of cobalamin; metabolism of essential amino acids (phenylalanine, lysine, valine, leucine, and isoleucine)

and nonessential amino acids (arginine, cysteine, and tyrosine); and in the pentose phosphate pathway (fig. S3, A and B; table S4, B to G; and table S5). Follow-up targeted tandem mass spectrometry (MS/MS)-based analysis of amino acids in sera obtained at the time mice were killed demonstrated significant increases in branched-chain amino acids (BCAA: Val and Leu/Ile), as well as other amino acids (Met, Ser, and Gly), plus trends to increase (Phe, Tyr, and Ala), in recipients of microbiota from obese compared with lean co-twins in discordant twin pairs DZ1 and MZ4 (tables S1D and S6A). These specific amino acids, as well as the magnitude of their differences, are remarkably similar to elevations in BCAA and related amino acids reported in obese and insulin-resistant versus lean and insulin-sensitive humans (25). This finding suggested that the gut microbiota from obese subjects could influence metabolites that characterize the obese state.

In contrast, the transplanted microbiomes from lean co-twins exhibited higher expression of genes involved in (i) digestion of plant-derived polysaccharides [e.g., α -glucuronidase (EC 3.2.1.139), α -L-arabinofuranosidase (EC 3.2.1.55)]; (ii) fermen-

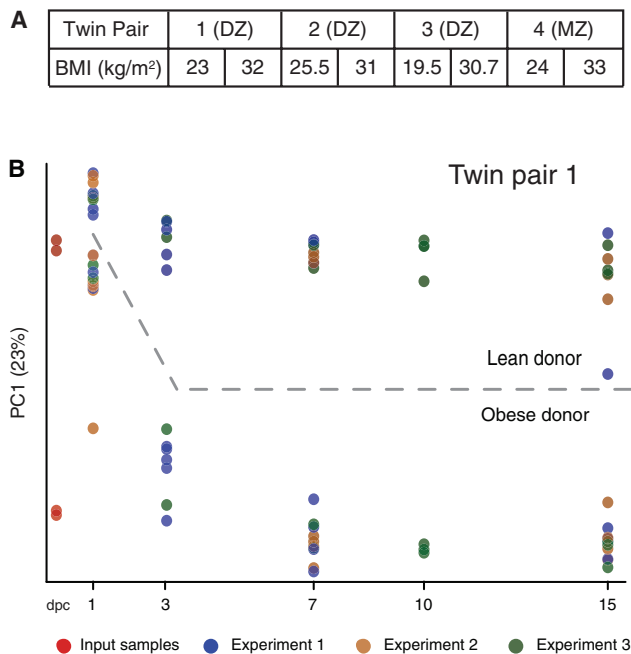
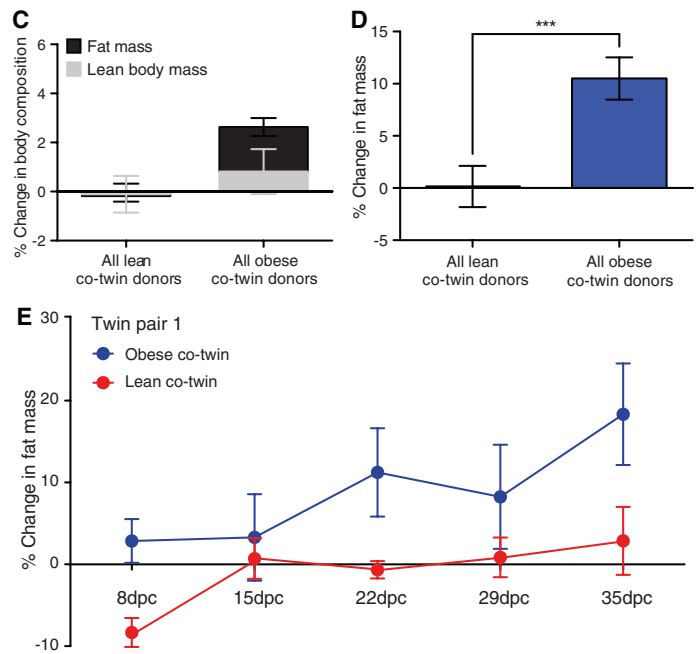


Fig. 1. Reliable replication of human donor microbiota in gnotobiotic mice. (A) Features of the four discordant twin pairs. (B) Assembly of bacterial communities in mice that had received intact and uncultured fecal microbiota transplants from the obese and lean co-twins in DZ pair 1. Principal coordinates analysis plot of principal coordinate 1 (PC1) based on an unweighted UniFrac distance matrix and 97%ID OTUs present in sampled fecal communities. Circles correspond to a single fecal sample obtained at a given time point from a given mouse and are colored according to the experiment ($n = 3$ independent experiments). Note that assembly is reproducible within members of a group of mice that have received a given microbiota, as well as between experiments. (C) Body composition, defined by QMR, was performed 1 day and 15 dpc of each mouse in each recipient group. Mean values (\pm SEM) are plotted for the percent increase in fat mass and lean body mass at 15 dpc for all recipient mice of each of the four obese co-twins' or lean co-twins' fecal microbiota, normalized to the



initial body mass of each recipient mouse. A two-way ANOVA indicated that there was a significant donor effect ($P \leq 0.05$), driven by a significant difference in adiposity and total body mass between mice colonized with a lean or obese co-twin donor's fecal microbiota (adjusted $P \leq 0.05$; Šidák's multiple comparison test). (D) Mean values (\pm SEM) are plotted for the percent change in fat mass at 15 dpc for all recipient mice of each of the four obese co-twins' or lean co-twins' fecal microbiota. Data are normalized to initial fat mass ($n = 3$ to 12 animals per donor microbiota; 51 to 52 mice per BMI bin; total of 103 mice). *** $P \leq 0.001$, as judged by a one-tailed unpaired Student's t test. (E) More prolonged time course study for recipients of fecal microbiota from co-twins in discordant DZ pair 1 (mean values \pm SEM plotted; $n = 4$ mice per donor microbiota). The difference between the gain in adiposity calculated relative to initial fat mass (1 dpc) between the two recipient groups of mice is statistically significant ($P \leq 0.001$, two-way ANOVA).

tation to butyrate [acetyl-CoA C-acetyltransferase (EC 2.3.1.9), 3-hydroxybutyryl-CoA dehydrogenase (EC 1.1.1.157), 3-hydroxybutyryl-CoA dehydratase (EC 4.2.1.55), butyryl-CoA dehydrogenase (EC 1.3.8.1)] (fig. S3, C and D); and (iii) fermentation to propionate [succinate dehydrogenase (EC 1.3.99.1), phosphoenolpyruvate carboxykinase (EC 4.1.1.32), methylmalonyl-CoA mutase (EC 5.4.99.2)] (table S4A). Follow-up gas chromatography–mass spectrometry (GC-MS) of cecal contents confirmed that levels of butyrate and propionate were significantly increased and that levels of several mono- and disaccharides significantly decreased in animals colonized with lean compared with obese co-twin gut communities ($P \leq 0.05$, unpaired Student's *t* test) (fig. S4, A and B, and table S6B). Procrustes analysis, using a Hellinger distance matrix (26), revealed significant correlations between taxonomic structure [97% identity (97%ID) threshold for defining distinct operational taxonomic units (OTU) in fecal samples], transcriptional profiles (enzyme representation in fecal mRNA populations), and metabolic profiles (GC-MS of cecal samples), with separation of groups based on donor microbiota and BMI (Mantel test, $P \leq 0.001$) (fig. S5).

These results suggest that, in this diet context, transplanted microbiota from lean co-twins had a greater capacity to breakdown and ferment polysaccharides than the microbiota of their obese co-twins. Previous reports have shown that increased microbial fermentation of nondigestible starches is associated with decreased body weight and decreased adiposity in conventionally raised mice that harbor a mouse microbiota [e.g., refs. (27–29)].

Phenotypes Produced by Bacterial Culture Collections

We followed up these studies of transplanted, intact, and uncultured donor communities with a set of experiments involving culture collections produced from the fecal microbiota of one of the discordant twin pairs. Our goal was to determine whether cultured bacterial members of the co-twins' microbiota could transmit the discordant adiposity phenotypes and distinctive microbiota-associated metabolic profiles when transplanted into gnotobiotic mouse recipients that received the LF-HPP chow diet.

Collections of cultured anaerobic bacteria were generated from each co-twin in DZ pair 1 and subsequently introduced into separate groups of 8-week-old germ-free male C57BL/6J mice ($n = 5$ independent experiments; $n = 4$ to 6 recipient mice per culture collection per experiment). The culture collections stabilized in the guts of recipient mice within 3 days after their introduction [see (23); fig. S6, A to E; and table S7 for documentation of the efficient and reproducible capture of cultured taxa and their encoded gene functions between groups of recipient mice].

As in the case of uncultured communities, we observed a significantly greater increase in adiposity in recipients of the obese twin's culture collection compared with the lean co-twin's culture collection ($P \leq 0.02$, one-tailed unpaired Student's *t* test) (Fig. 2, A and B). Nontargeted GC-MS showed

that the metabolic profiles generated by the transplanted culture collections clustered with the profiles produced by the corresponding intact uncultured communities (fig. S6E). In addition, the fecal biomass of recipients of the culture collection from the lean twin was significantly greater than the fecal biomass of mice receiving the culture collection from her obese sibling; these differences were manifest within 7 days ($P \leq 0.0001$, two-way ANOVA) (fig. S7A).

Cohousing Ob and Ln Animals Prevents an Increased Adiposity Phenotype

Because mice are coprophagic, the potential for transfer of gut microbiota through the fecal-oral route is high. Therefore, we used cohousing to determine whether exposure of a mouse harboring a culture collection from the lean twin could prevent development of the increased adiposity phenotype and microbiome-associated metabolic profile of a cage mate colonized with the culture collection from her obese co-twin or vice versa. Five days after gavage, when each of the inoculated microbial consortia had stabilized in the guts of recipient animals, a mouse with the lean co-twin's culture collection was cohoused with a mouse with the obese co-twin's culture collection (abbreviated Ln^{ch} and Ob^{ch}, respectively). Control groups consisted of cages of dually housed recipients of the lean twin culture collection and dually housed recipients of the obese co-twin's culture collection ($n = 3$ to 5 cages per housing configuration per experiment; $n = 4$ independent experiments; each housing configuration in each experiment was placed in a separate gnotobiotic isolator) (Fig. 2A). All mice were 8-week-old C57BL/6J males. All were fed the same LF-HPP chow ad libitum that was used for transplants involving the corresponding uncultured communities. Bedding was changed before initiation of cohousing. Fecal samples were collected from all recipients 1, 2, 3, 5, 6, 7, 8, 10, and 15 days after gavage. Body composition was measured by QMR 1 and 5 days after gavage, and after 10 days of cohousing.

Ob^{ch} mice exhibited a significantly lower increase in adiposity compared with control Ob animals that had never been exposed to mice harboring the lean co-twin's culture collection ($P \leq 0.05$, one-tailed unpaired Student's *t* test). Moreover, the adiposity of these Ob^{ch} animals was not significantly different from Ln controls ($P > 0.05$, one-tailed unpaired Student's *t* test) (Fig. 2B). In addition, exposure to Ob^{ch} animals did not produce a significant effect on the adiposity of Ln^{ch} mice: Their adiposity phenotypes and fecal biomass were indistinguishable from dually housed Ln controls (Fig. 2B; and fig. S7, B and C). Cohousing caused the cecal metabolic profile of Ob^{ch} mice to assume features of Ln^{ch} and control Ln animals, including higher levels (compared with dually housed Ob controls) of propionate and butyrate and lower levels of cecal mono- and disaccharides, as well as BCAA and aromatic amino acids (Fig. 2, C and D, and fig. S8).

Principal coordinates analysis of unweighted UniFrac distances revealed that the fecal micro-

biota of Ob^{ch} mice were reconfigured so that they came to resemble the microbiota of Ln^{ch} cage mates. In contrast, the microbiota of the Ln^{ch} cage mates remained stable (fig. S9, A to C). We performed a follow-up analysis to identify species-level taxa that had infiltrated into and/or had been displaced from the guts of mice harboring the Ln and Ob culture collections. We did so by characterizing the direction and success of invasion. Microbial SourceTracker estimates, for every species-level taxon or 97%ID OTU, the Bayesian probability (P) of its being derived from each of a set of source communities (30). The fecal microbiota of Ln or Ob controls sampled 5 days after colonization were used as source communities to determine the direction of invasion. The fecal communities belonging to each Ln^{ch} and Ob^{ch} mouse were then traced to these sources. We defined the direction of invasion for these bacterial taxa, by calculating the log odds ratio of the probability of a Ln origin (PLn) or an Ob origin (POb) for each species-level taxon or 97%ID OTU, i , as follows:

$$\log_2 (PLn_i / POB_i)$$

A positive log odds ratio indicated that a species or 97%ID OTU was derived from a Ln source; a negative log odds ratio indicated an Ob source. An invasion score was calculated to quantify the success of invasion of each species or 97%ID OTU, i , into each cohousing group, j , as follows:

$$Invasion\ Score_{ij} = \log_2 \left(\frac{\bar{A}_{ij}}{\bar{B}_j} \right)$$

where \bar{A}_{ij} is the average relative abundance of taxon i in all fecal samples collected from group j after cohousing, and \bar{B}_j is its relative abundance in all samples taken from that group before cohousing.

The observed mean of the distribution of invasion scores for Ob^{ch} animals was significantly higher than that for dually housed Ob-Ob controls ($P \leq 0.0005$, Welch's two-sample *t* test) (fig. S10A). This was not the case for Ln^{ch} animals when compared with dually housed Ln-Ln controls ($P > 0.05$), which suggested that there was significant invasion of components of the Ln^{ch} microbiota into the microbiota of Ob^{ch} cage mates, but not vice versa. To quantify invasion further, we used the mean and standard deviation of the null distribution of invasion scores (defined as the scores from recipients of the Ln or Ob microbiota that had never been cohoused with each other) to calculate a z value and a Benjamini-Hochberg adjusted P value for the invasion score of each species in Ln^{ch} and Ob^{ch} mice. We conservatively defined a taxon as a successful invader if it (i) had a Benjamini-Hochberg adjusted $P \leq 0.05$, (ii) was represented in $\geq 75\%$ of Ob^{ch} or Ln^{ch} mice when sampled 7 and 10 days after initiation of cohousing, and (iii) had a relative abundance of $\leq 0.05\%$ before cohousing and $\geq 0.5\%$ in the fecal microbiota at the time mice were killed. We defined a taxon that was displaced from an animal's microbiota upon cohousing as having a relative

abundance $\geq 1\%$ in Ln^{ch} or Ob^{ch} mice before they were cohoused and a relative abundance $< 0.5\%$ after cohousing.

The direction and success of invasion are shown in Fig. 2E and table S8A. The most successful Ln^{ch} invaders of the Ob^{ch} microbiota were

members of the Bacteroidetes (rank order of their invasion scores: *Bacteroides cellulosilyticus*, *B. uniformis*, *B. vulgatus*, *B. thetaiotaomicron*,

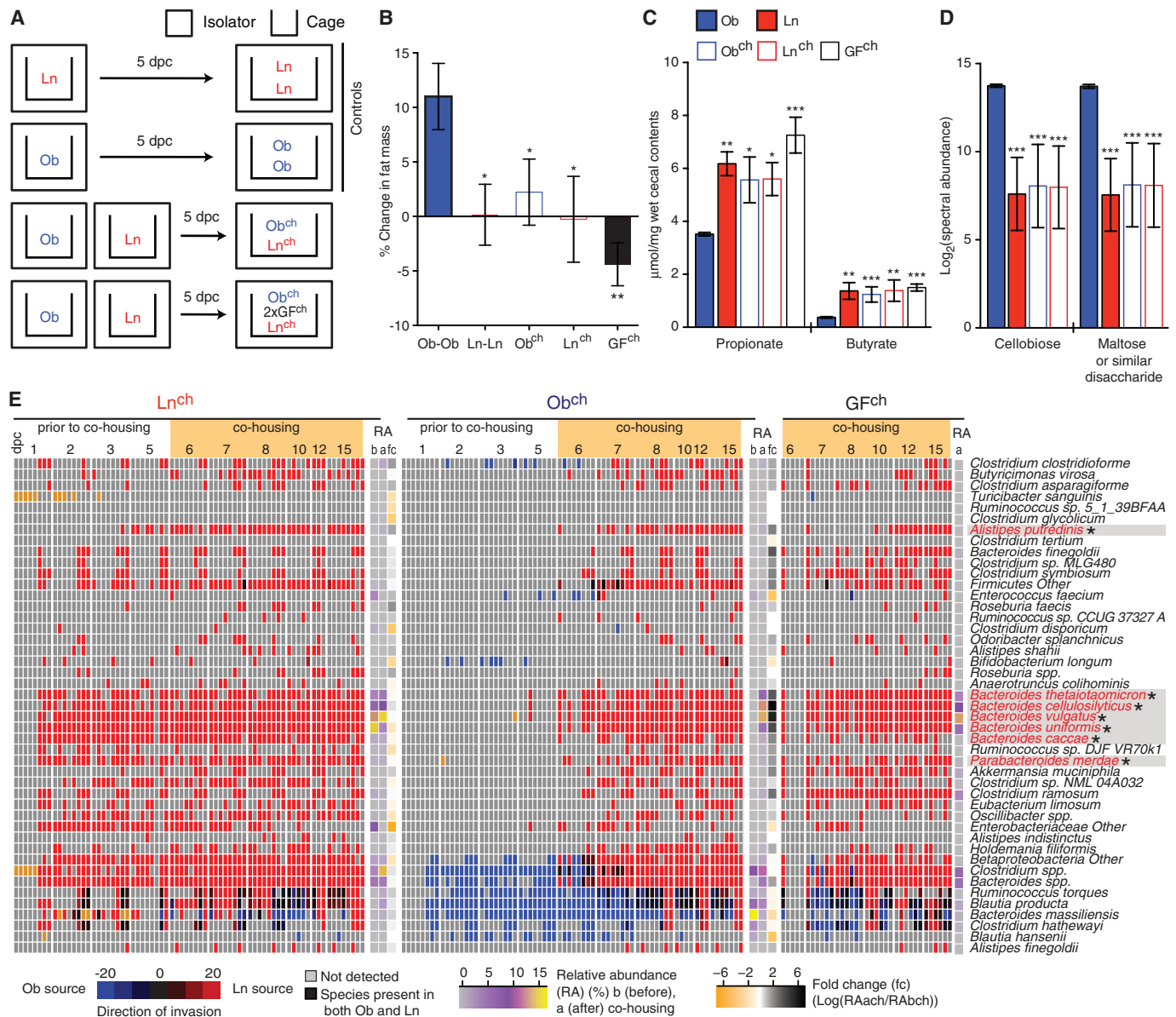


Fig. 2. Cohousing Ob^{ch} and Ln^{ch} mice transforms the adiposity phenotype of cage mates harboring the obese co-twin's culture collection to a lean-like state. (A) Design of cohousing experiment: 8-week-old, male, germ-free C57BL/6J mice received culture collections from the lean (Ln) twin or the obese (Ob) co-twin in DZ twin pair 1. Five days after colonization, mice were cohoused in one of three configurations: Control groups consisted of dually housed Ob-Ob or Ln-Ln cage mates; the experimental group consisted of dually housed Ob^{ch}-Ln^{ch} cage mates (data shown from five cages per experiment; two independent experiments) or Ob^{ch}-Ln^{ch}-GF^{ch}-GF^{ch} cage mates ($n = 3$ cages per experiment). All mice were fed a LF-HPP diet. (B) Effects of cohousing on fat mass. Changes from the first day after cohousing to 10 days after cohousing were defined using whole-body QMR. * $P < 0.05$, ** $P < 0.01$ compared with Ob-Ob controls, as defined by one-tailed unpaired Student's t test. (C) Targeted GC-MS analysis of cecal short-chain fatty acids. Compared with Ob-Ob controls, the concentrations of propionate and butyrate were significantly higher in the ceca of Ob^{ch}, Ln-Ln, Ln^{ch}, and GF^{ch} mice. (D) Nontargeted GC-MS analysis of cecal levels of cellobiose and "maltose or a similar disaccharide." * $P < 0.05$; ** $P < 0.01$; *** $P < 0.005$. (E) Evidence that bacterial species from the Ln^{ch}

microbiota invade the Ob^{ch} microbiota. Shown are SourceTracker-based estimates of the proportion of bacterial taxa in a given community sampled from a cage mate. For Ob^{ch}-Ln^{ch} cohousing experiments, Ob^{ch} and Ln^{ch} microbiota were designated as sink communities, whereas the gut microbiota of Ob-Ob and Ln-Ln controls (at 5 dpc) were considered source communities. Red indicates species derived from the Ln^{ch} gut microbial community. Blue denotes species derived from the Ob^{ch} microbiota. Black denotes unspecified source (i.e., both communities have this species), whereas orange indicates an uncertain classification by the SourceTracker algorithm. "Other" after a genus name means unclassified. An asterisk placed next to a species indicates that it is a successful invader as defined in the text. Average relative abundance (RA) in the fecal microbiota is shown before cohousing (b, at 5 dpc) and after cohousing (a, at 15 dpc). The average fold-change (fc) in relative abundance for a given taxon, for all time points before and after cohousing is shown (excluding the first 2 days immediately after gavage of the microbiota and immediately after initiation of cohousing). Note that only taxa with significant changes in relative abundance between samples collected before and samples collected after cohousing are shown. For a full accounting of all taxa, see table S8A.

B. caccae, *Alistipes putredinis*, and *Parabacteroides merdae*). Invasiveness exhibited specificity at the 97%ID OTU level (fig. S11). In contrast, cohousing did not result in significant invasion of Ln^{ch} intestines with members of the Ob^{ch} microbiota.

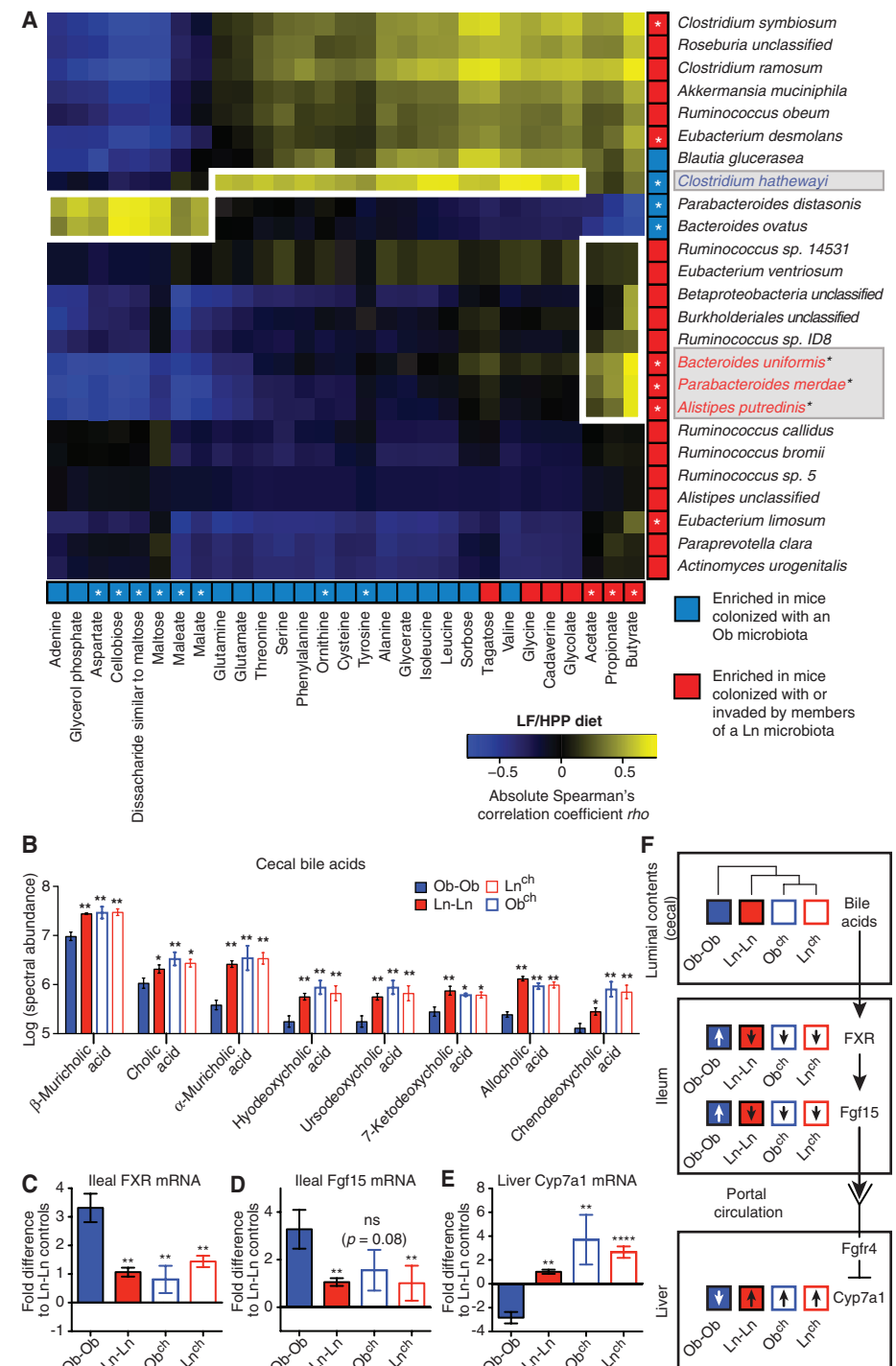
In macroecosystems, successful invaders are often more likely to become established if they are from divergent taxa that do not share a niche with members of the native entrenched community (31, 32). We used the Net Relatedness Index [NRI (33)] to show that Ln and Ob communities

have different phylogenetic structures and that the patterns of phylogenetic clustering and dispersion of Ob, but not Ln microbiota, change as a consequence of cohousing. Specifically fecal Ln, Ln^{ch}, and Ob^{ch} communities had a negative NRI, which indicates that the community is more phylogenetically dispersed than Ob controls. Furthermore, the fecal communities of Ln^{ch} and Ob^{ch} animals had significantly more shared branch length with each other after cohousing compared with before cohousing [for a description of calculations and interpretation, see (23), fig. S9E,

and fig. S12]. Together, these patterns of phylogenetic overdispersion and increased shared branch length in cohoused Ln^{ch} and Ob^{ch} animals led us to hypothesize that Bacteroides in the Ln^{ch} community were efficient invaders of Ob^{ch} communities because they were able to occupy unoccupied niches in Ob^{ch} intestines. Note that increased representation of Bacteroidetes has been documented in several independent studies of the gut microbiota of conventionally raised lean mice compared with mice having genetic- or diet-induced obesity (34, 35).

Fig. 3. Effect of cohousing on metabolic profiles in mice consuming the LF-HPP diet.

(A) Spearman's correlation analysis of cecal metabolites and cecal bacterial species-level taxa in samples collected from Ob^{ch}, Ln^{ch}, GF^{ch}, Ln39^{ch}, and Ob^{ch}Ln39^{ch} cage mates and from Ob-Ob and Ln-Ln controls (correlations with $P \leq 0.0001$ are shown). Taxonomic assignments were made using a modified taxonomy from the National Center for Biotechnology Information (of the U.S. National Institutes of Health) (23). Bacterial species and cecal metabolites enriched in animals colonized with either the Ln or Ob culture collections are colored red and blue, respectively. An asterisk in the colored box indicates that a taxon or metabolite is significantly enriched in mice colonized with Ln (red) or Ob (blue) culture collections. Bacterial species colored red denote significant invaders from Ln^{ch} mice into the gut microbiota of Ob^{ch} cage mates. (B) Cecal bile acids measured by UPLC-MS. Note that levels are plotted as log-transformed spectral abundances. Significance of differences relative to Ob-Ob controls were defined using a two-way ANOVA with Holm-Šidák's correction for multiple hypotheses; * $P \leq 0.05$; ** $P \leq 0.01$. (C and D) QPCR assays of FXR and Fgf15 mRNA levels in the distal ileum. Data are normalized to Ln-Ln controls. (E) QPCR of hepatic Cyp7a1 mRNA, normalized to Ln-Ln controls. * $P \leq 0.05$; ** $P \leq 0.01$; **** $P \leq 0.001$ (defined by one-tailed, unpaired Student's t test using Ob-Ob mice as reference controls). (F) Correlating cecal bile acid profiles with the FXR-Fgf15-Cyp7A signaling pathway in the different groups of mice. (Top) The dendrogram highlights the differences in the profiles of 37 bile acid species between Ob-Ob controls and the other three treatment groups (table S11). The dendrogram was calculated using the Bray-Curtis dissimilarity index and the average relative abundance of each bile acid species among all mice belonging to a given treatment group.



Control experiments involving cohousing a germ-free (GF^{ch}) mouse with an Ob mouse 5 days after transplantation of the complete culture collection from the obese co-twin demonstrated effective transmission of the Ob adiposity phenotype to the GF cage mate (defined by epididymal fat pad weight as a percentage of total body weight; $P > 0.05$, comparing GF^{ch}-Ob and Ob^{ch}-GF cage mates with a two-tailed unpaired Student's t test). The adiposity (epididymal fat pad weights) of the GF^{ch}-Ob cage mate was significantly greater compared with GF-GF controls [$1.4 \pm 0.1\%$ of body weight (Ob^{ch}-GF); $1.4 \pm 0.05\%$ (GF^{ch}-Ob); $1.5 \pm 0.05\%$ (Ob-Ob controls) versus $0.8 \pm 0.06\%$ (GF-GF controls); $P < 10^{-4}$, two-tailed unpaired Student's t test between GF^{ch}-Ob and GF-GF controls; $n = 6$ GF-GF, 8 Ob-Ob, and 10 GF^{ch}-Ob-Ob^{ch}-GF]].

In separate experiments, we cohoused two GF animals together with one Ln and one Ob animal, 5 days after colonization of Ln and Ob mice (repeated in three separate cages, each cage in a separate isolator). As with previous experiments, bedding was changed before initiation of cohousing. The GF "bystanders" did not develop increased adiposity phenotypes and manifested cecal metabolic profiles and fecal biomass characteristics of their Ln^{ch} cage mates and Ln controls (Fig. 2, B to E, and fig. S7F). In the initial phase of cohousing (days 1 to 2), the microbiota of GF^{ch} mice in each cage resembled that of noncohoused Ob-Ob controls (fig. S9D). By the next day, the

microbiota of each ex-GF^{ch} animal had undergone a dramatic change in composition, with $94.8 \pm 0.4\%$ of taxa now derived from their Ln^{ch} cage mate (defined by SourceTracker; see table S8A for log odds ratio scores). The most prominent invaders were the same prominent invaders from the Ln^{ch} microbiota described above (i.e., all of the Bacteroidales) (Fig. 2E). We concluded that these Ln-derived taxa had greater fitness in the guts of C57BL/6J mice consuming this diet, and had a "dominant-negative" effect on host adiposity.

Changes in the Cecal Metatranscriptome and Metabolome of Ob^{ch} Animals

Cecal samples collected at the time mice were killed from Ln^{ch}, Ob^{ch}, and control Ob and Ln animals were subjected to microbial RNA-Seq. Reads were assigned to ECs as above, and Euclidean distances were calculated from the EC matrix. The results revealed that the metatranscriptomes of Ob^{ch} animals were significantly more similar to those of their Ln^{ch} cage mates and Ln controls than to Ob controls, consistent with a functional transformation of the Ob^{ch} microbiota to a leanlike state as a consequence of invasion of the Ln taxa ($P \leq 0.0001$ as measured by a one-way ANOVA, with Holm-Šidák's correction for multiple hypotheses) (fig. S13). The majority (55.9%) of ECs that were enriched in the cecal metatranscriptomes of Ob^{ch} mice, compared with dually housed Ob-Ob controls, were also significantly

enriched in dually housed Ln-Ln versus Ob-Ob controls, including ECs that participate in carbohydrate metabolism and protein degradation. The latter encompassed five enzymes involved in the KEGG pathway for degradation of the BCAA valine, leucine, and isoleucine (transcripts encoding EC 1.2.4.4; EC 2.6.1.42; EC 5.1.99.1, and EC 6.4.1.3, which map to the genomes of invading members of the *Bacteroides*, and EC 4.2.1.17, which maps to members of Clostridiaceae) (table S9). The increased expression of genes involved in BCAA degradation is consistent with the reduced cecal levels of BCAA observed in Ln-Ln, Ln^{ch} and Ob^{ch} animals versus Ob-Ob controls (fig. S8). These results are consistent with the notion that invasion by *Bacteroides* increases the efficiency of BCAA degradation in the gut, reducing production of BCAA and related metabolites by the microbiome and contributing to decreased circulating levels of BCAA in the host. As with transplanted, intact, and uncultured microbiota from the discordant twin pairs, targeted MS/MS analysis confirmed that Ob-Ob controls had a global increase in serum levels of BCAAs, as well as higher levels of Met, Ser, Gly, Phe, Tyr, and Ala compared with Ln-Ln controls ($P \leq 0.05$, matched one-way ANOVA) (table S10). However, after 10 days of cohousing, Ob^{ch} animals did not exhibit a statistically significant reduction in serum BCAA levels compared with Ob-Ob controls, although levels in Ln^{ch} cage mates were significantly

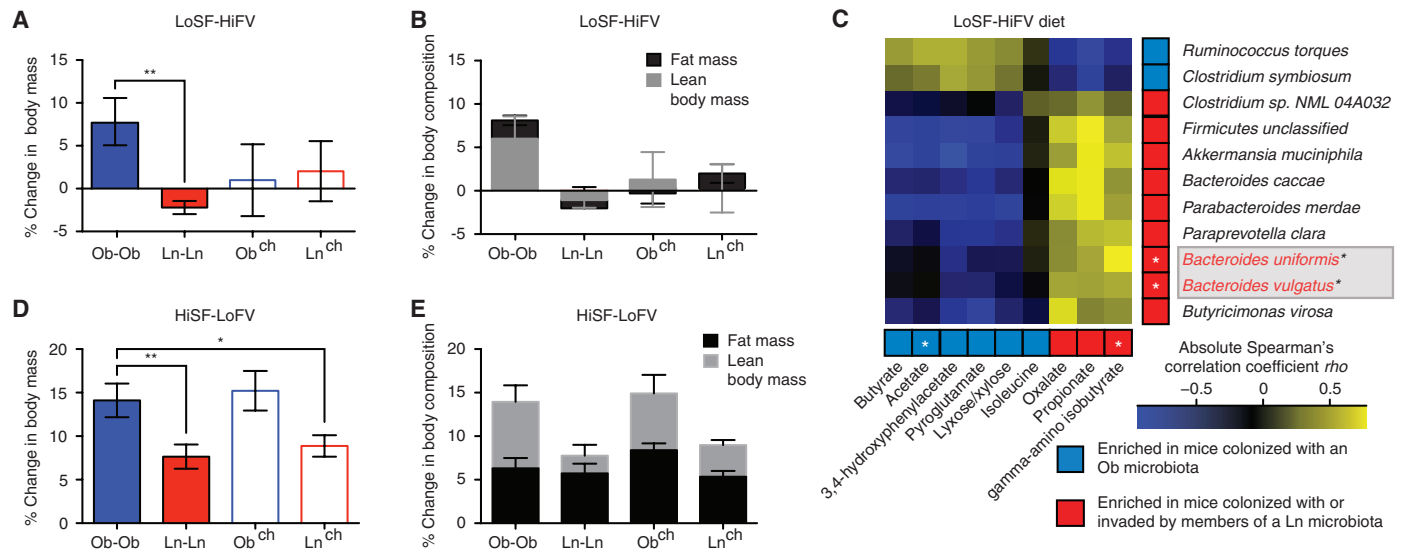


Fig. 4. Effects of NHANES-based LoSF-HiFV and HiSF-LoFV diets on bacterial invasion, body mass and metabolic phenotypes. (A and B) Mean \pm SEM percent changes in total body mass (A) and body composition [fat and lean body mass, normalized to initial body mass on day 4 after gavage (B)] occurring between 4 and 14 days after colonization with culture collections from the Ln or Ob co-twin in DZ pair 1. Cohousing Ln and Ob mice prevents an increased body mass phenotype in Ob^{ch} cage mates fed the representative LoSF-HiFV human diet ($n = 3$ to 5 cages per treatment group; 26 animals in total). ** $P \leq 0.01$, based on a one-way ANOVA after Fisher's least significant difference test (also see table S14 for statistics). (C) Spearman's correlation analysis between bacterial species-level taxa and metabolites in cecal samples collected from mice colonized with culture collections from DZ twin pair 1 Ln and Ob co-twins and fed a LoSF-HiFV diet. Red and blue squares indicate metabolites or

taxa that are significantly enriched in samples collected from dually housed Ln-Ln or Ob-Ob controls respectively. An asterisk in the colored box indicates that a taxon or metabolite is significantly enriched in mice colonized with Ln (red) or Ob (blue) culture collections. (D and E) Mean \pm SEM of changes in body mass and body composition in mice colonized with intact uncultured microbiota from DZ twin pair 2 and fed the representative HiSF-LoFV human diet. Ob-Ob controls have greater total and lean body mass than Ln-Ln controls, but this phenotype is not rescued in Ob^{ch} animals (see table S14 for statistics). * $P < 0.05$, ** $P \leq 0.01$ based on a one-way ANOVA. Note that the HiSF-LoFV diet produces a significantly greater increase in body mass, specifically fat mass, in mice harboring the lean co-twins microbiota (Ln-Ln and Ln^{ch}) than when they are fed the LoSF-HiFV diet [see (A) versus (D), and (B) versus (E); two-way ANOVA with Holm-Šidák's correction for multiple hypotheses].

cantly lower than in Ob-Ob controls and not different from Ln controls (table S10). More complete understanding of the contributions of the gut microbial community to Ob-associated metabolic phenotypes will require detailed, long-term, time-series studies of microbial and host transcriptomes and metabolomes.

Significant correlations between cecal metabolite levels and bacterial species represented in the microbiota of Ob-Ob, Ln-Ln, Ln^{ch}, Ob^{ch} and GF^{ch} mice consuming the LF-HPP diet are summarized in Fig. 3A (defined by asymptotic *P* values for all Spearman's correlations, corrected for multiple hypotheses using the Benjamini-Hochberg procedure). For example, BCAA and the products of amino acid metabolism were positively correlated with *Clostridium hathewayi* (Fig. 3A). This member of the Firmicutes represented an average of 2.54% of the Ob fecal microbiota before cohousing; its relative abundance was significantly reduced in Ob^{ch} animals, and it was not able to successfully invade the microbiota of Ln^{ch} cage mates (Figs. 2E and 3A and table S8A).

Three members of the Bacteroidetes, *B. uniformis*, *Parabacteroides merdae*, and *A. putredinis*, which were prominent invaders of the Ob^{ch} gut, positively correlated with cecal acetate, propionate, and butyrate levels. Whereas members of these species generate acetate

and propionate, their ability to produce butyrate has not been reported. Their positive association with butyrate levels could be due to interspecies acetate cross-feeding with butyrate-producing taxa (36, 37). The negative correlation between adiposity and cecal butyrate and propionate concentrations in Ln^{ch}, Ob^{ch}, and GF^{ch} microbiota ($r = -0.49$ and -0.45 , respectively, $P \leq 0.05$) is consistent with previous studies claiming a role for these short-chain fatty acids in influencing host energy balance (38, 39).

The gut microbiota affects the composition and relative abundance of bile acids species through a variety of metabolic transformations (40, 41). Ultra-performance liquid chromatography–mass spectrometry (UPLC-MS) analysis of 37 bile acid species in cecal samples obtained from Ln-Ln, Ob-Ob, Ob^{ch}, and Ln^{ch} mice revealed significantly lower levels of eight bile acids in Ob-Ob compared with Ln-Ln controls (Fig. 3B). Cohousing rescued these differences, with Ob^{ch} mice having bile acid profiles that were more similar to Ln-Ln than to Ob-Ob controls and not significantly different from Ln^{ch} cage mates ($n = 5$ to 6 mice per group; see table S11 for all bile acids measured that exhibit significant differences between Ob-Ob and Ln-Ln controls).

Bile acids can have direct metabolic effects on the host via the nuclear farnesoid X receptor (FXR)

(42). Intestinal FXR mediates intestinal fibroblast growth factor 15 (Fgf15) production. Fgf15, secreted by the gut epithelium and delivered to hepatocytes via the portal circulation, acts through fibroblast growth factor receptor 4 (*Fgfr4*) to inhibit expression of the rate-limiting enzyme in bile acid biosynthesis, cholesterol 7- α -hydroxylase (*Cyp7a1*) (Fig. 3, C to F) (43). Engineered FXR deficiency in leptin-deficient mice protects against obesity and improves insulin sensitivity (42). Overexpression of *Cyp7a1* in the livers of transgenic mice also prevents diet-induced obesity and insulin resistance (44). Sequestering bile acids with the drug colestevam lowers blood sugar in humans with type 2 diabetes (45). Quantitative reverse transcription polymerase chain reaction (qRT-PCR) analysis disclosed that, compared with Ln-Ln animals, Ob-Ob mice have increased FXR and Fgf15 mRNA levels in their distal small intestine (ileum) and decreased hepatic *Cyp7a1* expression. Ob^{ch} mice have expression profiles that are not significantly different from Ln-Ln controls (or Ln^{ch}) (Fig. 3, C to E). Differences in bile acid metabolism, in addition to the documented differences in carbohydrate fermentation by Ob compared with Ln microbial communities highlight some of the mechanisms that could contribute to the observed microbiota-mediated effects on body composition.

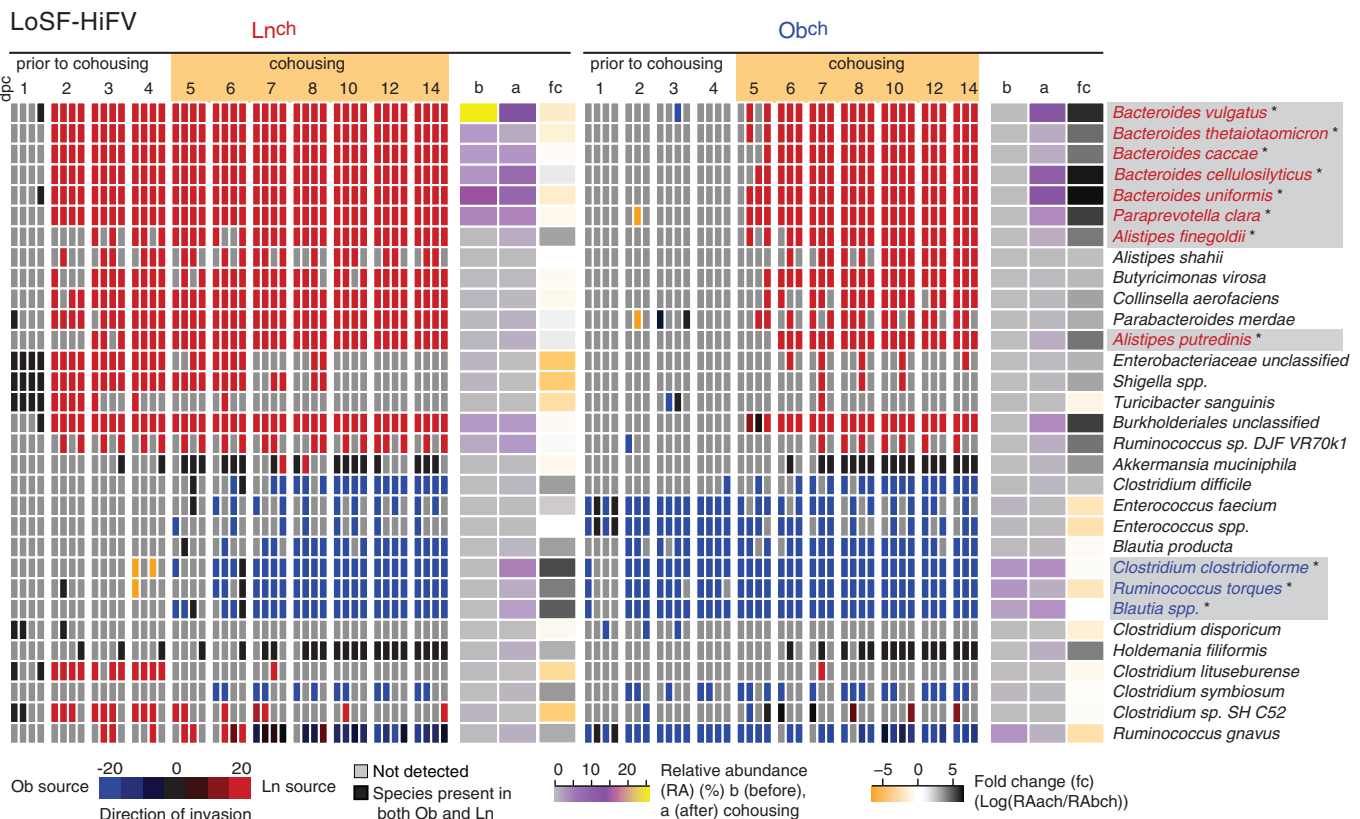


Fig. 5. Invasion analysis of species-level taxa in Ob^{ch} or Ln^{ch} mice fed the NHANES-based LoSF-HiFV diet. Red indicates species derived from the Ln^{ch} gut microbial community. Blue denotes species derived from the Ob^{ch} microbiota. The mean relative abundance of each species-level taxon before

(b: 3 and 4 dpc) and after (a: 8, 10 and 14 dpc) cohousing is noted. Average fold-change (fc) in relative abundance of taxa before and after colonization was defined as in the legend to Fig. 2E. An asterisk (*) denotes bacterial species that satisfy our criteria for classification as successful invaders (see text).

Taxa-Specific Effects on Body Composition and Metabotype

We subsequently colonized GF mice with a consortium of 39 sequenced taxa (97% ID OTUs) from the lean co-twin's culture collection; 22 OTUs from *Bacteroides*, including *B. cellulosilyticus*, *B. vulgatus*, *B. thetaiotaomicron*, *B. caccae*, *B. ovatus*; 11 OTUs from *Ruminococcaceae* (one of the four family-level taxa that discriminate lean from obese), and six strains of *Collinsella aerofaciens* (richly endowed with genes involved in the acquisition and fermentation of diverse dietary carbohydrates) (see table S12 for features of the 39 sequenced genomes). Five days after colonization with the 39 taxa, these Ln39 mice were cohoused with Ob mice. Control groups consisted of dually housed Ln-Ln and dually housed Ob-Ob animals (fig. S14A) ($n = 5$ cages of cohoused animals per group; two independent experiments). Mice harboring the 39-member consortium (Ln39^{ch}), when cohoused with Ob (Ob^{ch}Ln39) animals, remained lean (fig. S14, A and B). However, Ln39^{ch} animals were not able to confer protection against an increase in adiposity of their Ob^{ch} cage mates, nor did they exhibit a significant increase in their cecal butyrate levels (figs. S14, B and C and S7, D and E). Even though some species like *B. cellulosilyticus* and *B. vulgatus* from the Ln39^{ch} microbiota exhibited significant invasion into the microbiota of Ob^{ch}Ln39 cage mates, there was an overall decrease in invasion efficiency for members of the Ln39 consortia compared with those in the complete Ln culture collection [the mean of the distribution of invasion scores for the Ob^{ch}Ln39 microbiota was not significantly different from Ob-Ob controls ($P > 0.05$, Welch's two-sample t test)] (fig. S10B, table S8B). These findings illustrate how invasiveness and adiposity are dependent on community context.

Diet-Specific Effects

To define the effects of diet on Ln and Ob microbiota-mediated transmission of body composition and metabolic phenotypes, we constructed a diet made with foods that characterize diets representing the lower tertile of consumption of saturated fats and the upper tertile of consumption of fruits and vegetables reported in 1-day recalls by participants in the U.S. National Health and Nutrition Examination Survey (NHANES) during the period 2003–2008 [table S13 (23)]. Mice fed this low-saturated fat, high fruits and vegetables (LoSF-HiFV, ~33% kcal of fat per 100 g) NHANES-based diet were colonized with either the Ln or Ob human culture collections and subsequently cohoused. Dually housed Ln-Ln and Ob-Ob animals served as reference controls ($n = 3$ to 5 cages per housing configuration; two independent experiments). Ob-Ob cage mates consuming the LoSF-HiFV diet had significantly increased body mass compared with Ln-Ln cage mates, which reflected a significant increase in both adipose and lean body mass (one-way unpaired Student's t test; $P \leq 0.001$) (Fig. 4, A and B, and table S14).

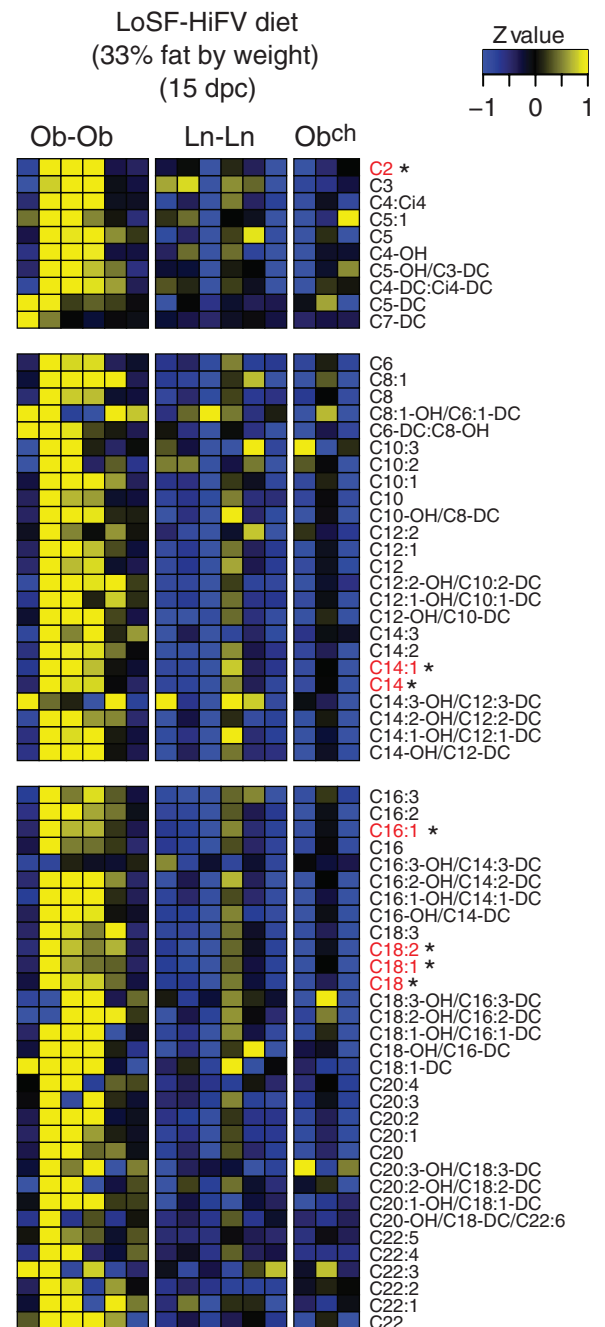
Cohousing prevented development of an Ob body composition phenotype in Ob^{ch} animals (Fig. 4, A and B).

We used 16S rRNA analysis of fecal samples collected on days 1 to 8, 10, 12, and 14 after gavage of the culture collections, and it revealed that this rescue was accompanied by invasion of taxa from Ln^{ch} to Ob^{ch} cage mates ($P < 10^{-6}$; Welch's two sample t test comparing the mean of the distributions of invasion scores between Ob-Ob controls and Ob^{ch} animals) with the most invasive species being members of *Bacteroides* (i.e., *B. uniformis*, *B. vulgatus*, and *B. cellulosilyticus*) (Fig. 5; fig. S15, A to C; and fig. S10C). These species were also successful invaders in mice fed the LF-HPP

diet (Fig. 2E). As was the case with the LF-HPP mouse chow, fecal samples collected from Ln-Ln controls and from Ln^{ch} and Ob^{ch} animals fed the human (NHANES-based) LoSF-HiFV diet had significantly greater microbial biomass compared with Ob-Ob controls (two-way ANOVA, $P \leq 0.001$ after Holm-Šidák's correction for multiple hypothesis). Moreover, fecal microbial biomass in Ob^{ch} and Ln^{ch} animals was not significantly different (not shown).

Significant correlations between cecal metabolites and cecal bacterial taxa in mice fed a LoSF-HiFV diet are summarized in Fig. 4C. As in mice fed a LF-HPP diet, the invasive species *B. uniformis* and *B. vulgatus* were significantly and positively

Fig. 6. Acylcarnitine profile in the skeletal muscle of mice colonized with the Ob or Ln culture collections from DZ twin pair 1 and fed the LoSF-HiFV diet. Each column represents a different animal and each row a different acylcarnitine. The identities and levels of these acylcarnitines were determined by targeted MS/MS (see table S15 for mean values \pm SEM for each treatment group). A two-way ANOVA with Holm-Šidák's correction was used to calculate whether the level of each acylcarnitine was significantly different between Ob-Ob and Ln-Ln, Ln^{ch}, or Ob^{ch} animals. * $P \leq 0.05$.



correlated with increased cecal propionate levels in Ln-Ln, Ob^{ch}, and Ln^{ch} animals compared with Ob-Ob controls.

Obesity-related insulin resistance has been associated with broad-scale accumulation of acylcarnitines in skeletal muscle (46, 47). Maneuvers that resolve the acylcarnitine accumulation in muscle, including knockout of the malonylCoA decarboxylase gene (*Mlycd*) or overexpression of carnitine acyltransferase (*Crat*), also resolve the insulin-resistance phenotype in mice (47, 48). Therefore, we used targeted MS/MS to measure 60 acylcarnitine species (C2 to C22) in liver, skeletal muscle, and serum (table S15, A to C). With the LF-HPP mouse chow (4% fat by weight), Ob-Ob animals had significantly higher levels of hepatic short-chain acylcarnitines (C2, C4:C4i, and C4-OH) compared with Ln-Ln mice (fig. S16; two-way ANOVA after Holm-Šidák's correction). The differences in short-chain acylcarnitines were rescued in Ob^{ch} animals, which resembled Ln-Ln controls ($n = 5$ animals per treatment group).

Ob-Ob controls fed the LoSF-HiFV diet (33% fat by weight) also had clear increases in accumulation of a group of even-, long-chain acylcarnitines (C14, C14:1, C16, C16:1, C18, C18:1, and C18:2) in their liver and skeletal muscle compared with Ln-Ln controls [multivariate ANOVA (MANOVA), $P \leq 0.001$; $n = 3$ to 6 animals per treatment group]. Cohousing Ln and Ob animals rescued this metabolic phenotype in the skeletal muscle and liver (and cecum) of Ob^{ch} mice (i.e., there was no statistically significant difference compared with Ln-Ln controls) (Fig. 6, fig. S16, and table S15). There were no significant differences in accumulation of these acylcarnitines in the plasma of Ob-Ob, Ln-Ln, and cohoused animals (table S15, B and C). Together, these results suggest that the gut microbiome influences systemic lipid metabolism.

Because these findings raised the possibility that the Ob microbiome is capable of conferring muscle insulin resistance at least in the context of a human (LoSF-HiFV) diet, we subjected Ob-Ob and Ln-Ln animals to a glucose tolerance test 15 days after colonization with their human donor's gut culture collections. An increase in serum glucose concentration was observed 15 min after intraperitoneal injection of glucose in Ob-Ob animals (means \pm SEM; 338.5 ± 11.07 mg/dl in Ob-Ob animals versus 304.6 ± 17.78 mg/dl in Ln-Ln animals; $P = 0.06$, unpaired Student's *t* test; $n = 10$ to 11 animals per group). No significant differences in serum insulin concentrations between these groups were documented at 30 min after glucose was administered, nor did we observe significant differences in insulin signaling in liver and skeletal muscle, defined by levels of immunoreactive Akt phosphorylated at Thr³⁰⁸ and the Akt substrate AS160 phosphorylated at Thr⁶⁴² measured 3 min after an insulin bolus (23). We concluded that the elevation in skeletal muscle long-chain acylcarnitines observed in mice colonized for just 15 days with an Ob culture collection and consuming the LoSF-HiFV diet is associated with mild glucose intolerance and may be an early

manifestation of the pathobiologic effects of obese microbiota on host physiology and metabolism. More complete time-course studies will be required to test if this lesion in glucose homeostasis will evolve into full-fledged insulin resistance with longer exposure to Ob microbiota.

To determine whether the effects exerted by diet on the invasive potential of members from the Ln microbiota were specific to the culture collections prepared from members of discordant twin pair 1 or robust to other Ln co-twin microbiota, we fed the LoSF-HiFV diet to mice colonized with intact uncultured fecal microbiota from members of discordant twin pair 2. Cohousing experiments performed using the same experimental design described above revealed invasion of the communities of Ob^{ch} animals by bacterial species from their Ln^{ch} cage mates, most notably members of the Bacteroidetes (figs. S10D and S17A, see table S8D for invasion scores).

In follow-up experiments, separate groups of germ-free mice colonized with intact uncultured microbiota from discordant twin-pair 2 were fed a second NHANES-based diet made with foods that characterize U.S. diets representing the upper, rather than lower, tertile of consumption of saturated fats and the lower, rather than upper, tertile of consumption of fruits and vegetables (abbreviated HiSF-LoFV; 44% fat by weight). Significant differences in body composition were documented between Ob-Ob and Ln-Ln mice fed this diet. However, cohousing of Ln and Ob mice failed to attenuate or block development of an increased body mass phenotype in Ob^{ch} cage mates ($n = 5$ to 11 animals per housing configuration) (Fig. 4, D and E). Remarkably, there was a lack of significant invasion of members of the Ln^{ch} microbiota into the guts of Ob^{ch} cage mates (figs. S10E and S17B and table S8E). If biased fecal pellet consumption was the underlying mechanism leading to invasion of members of the Ln microbiota into the guts of Ob^{ch} mice in the cohousing experiments, it would have to be diet- and microbiota-dependent. Together, these results emphasize the strong microbiota-by-diet interactions that underlie invasion and illustrate how a diet high in saturated fats and low in fruits and vegetables can select against human gut bacterial taxa associated with leanness.

Prospectus

The findings described above provide a starting point for future studies that systematically test the effects of specified diet ingredients on microbiota-associated body composition and metabolic phenotypes (e.g., components that when added or subtracted restore invasiveness of specific members of the microbiota in the context of the HiSF-LoFV diet). A benefit of using the approach described in this report is that the target human population embodying a phenotype of interest is integrated into the animal model through selection of gut microbiota representative of that population and diets representative of their patterns of food consumption. Our finding that cul-

ture collections generated from human microbiota samples can transmit donor phenotypes of interest (body composition and metabolites) has a number of implications. If these derived culture collections can transmit a phenotype, the stage is set for studies designed to determine which culturable components of a given person's gut community are responsible. These tests can take the form of experiments where mice containing culture collections from donors with different phenotypes are cohoused and used to determine whether invasion by components of one community into another transforms the cage mate's phenotype and, correspondingly, the properties of the human microbial communities they harbor. Sequenced culture collections generated from human gut microbiota donors also provide an opportunity to model and further address basic issues such as the determinants of invasiveness including the mechanisms by which invasion is impacted by diet composition, as well as the mechanisms by which invading components affect microbial and host metabolism. This issue is important for identifying next-generation probiotics, prebiotics, or a combination of the two (synbiotics). Moreover, the ability to generate a culture collection, from an individual—whose composition is resolved to the gene level, whose properties can be validated in preclinical models, and whose "manufacture" is reproducible—may provide a safer and more sustainable alternative to fecal transplants for microbiome-directed therapeutics (18, 49).

References and Notes

1. P. B. Eckburg *et al.*, Diversity of the human intestinal microbial flora. *Science* **308**, 1635–1638 (2005). doi: [10.1126/science.1110591](https://doi.org/10.1126/science.1110591); pmid: [15831718](https://pubmed.ncbi.nlm.nih.gov/15831718/)
2. P. J. Turnbaugh *et al.*, A core gut microbiome in obese and lean twins. *Nature* **457**, 480–484 (2009). doi: [10.1038/nature07540](https://doi.org/10.1038/nature07540); pmid: [19043404](https://pubmed.ncbi.nlm.nih.gov/19043404/)
3. E. K. Costello *et al.*, Bacterial community variation in human body habitats across space and time. *Science* **326**, 1694–1697 (2009). doi: [10.1126/science.1177486](https://doi.org/10.1126/science.1177486); pmid: [19892944](https://pubmed.ncbi.nlm.nih.gov/19892944/)
4. J. Qin *et al.*, A human gut microbial gene catalogue established by metagenomic sequencing. *Nature* **464**, 59–65 (2010). doi: [10.1038/nature08821](https://doi.org/10.1038/nature08821); pmid: [20203603](https://pubmed.ncbi.nlm.nih.gov/20203603/)
5. J. Ravel *et al.*, Vaginal microbiome of reproductive-age women. *Proc. Natl. Acad. Sci. U.S.A.* **108** (Suppl. 1), 4680–4687 (2011). doi: [10.1073/pnas.1002611107](https://doi.org/10.1073/pnas.1002611107); pmid: [20534435](https://pubmed.ncbi.nlm.nih.gov/20534435/)
6. P. Gajer *et al.*, Temporal dynamics of the human vaginal microbiota. *Sci. Transl. Med.* **4**, 132ra52 (2012). doi: [10.1126/scitranslmed.3003605](https://doi.org/10.1126/scitranslmed.3003605)
7. T. Yatsunenko *et al.*, Human gut microbiome viewed across age and geography. *Nature* **486**, 222–227 (2012). pmid: [22699611](https://pubmed.ncbi.nlm.nih.gov/22699611/)
8. C. Huttenhower *et al.*, Structure, function and diversity of the healthy human microbiome. *Nature* **486**, 207–214 (2012). doi: [10.1038/nature11234](https://doi.org/10.1038/nature11234); pmid: [22699609](https://pubmed.ncbi.nlm.nih.gov/22699609/)
9. K. Faust *et al.*, Microbial co-occurrence relationships in the human microbiome. *PLoS Comput. Biol.* **8**, e1002606 (2012). doi: [10.1371/journal.pcbi.1002606](https://doi.org/10.1371/journal.pcbi.1002606); pmid: [22807668](https://pubmed.ncbi.nlm.nih.gov/22807668/)
10. M. G. Dominguez-Bello *et al.*, Delivery mode shapes the acquisition and structure of the initial microbiota across multiple body habitats in newborns. *Proc. Natl. Acad. Sci. U.S.A.* **107**, 11971–11975 (2010). doi: [10.1073/pnas.1002601107](https://doi.org/10.1073/pnas.1002601107); pmid: [20566857](https://pubmed.ncbi.nlm.nih.gov/20566857/)

11. J. J. Faith *et al.*, Succession of microbial consortia in the developing infant gut microbiome. *Science* **341**, 1237439 (2013).
12. S. Greenblum, P. J. Turnbaugh, E. Borenstein, Metagenomic systems biology of the human gut microbiome reveals topological shifts associated with obesity and inflammatory bowel disease. *Proc. Natl. Acad. Sci. U.S.A.* **109**, 594–599 (2012). doi: [10.1073/pnas.1116053109](https://doi.org/10.1073/pnas.1116053109); pmid: [22184244](https://pubmed.ncbi.nlm.nih.gov/22184244/)
13. M. L. Zupancic *et al.*, Analysis of the gut microbiota in the old order Amish and its relation to the metabolic syndrome. *PLoS ONE* **7**, e43052 (2012). doi: [10.1371/journal.pone.0043052](https://doi.org/10.1371/journal.pone.0043052); pmid: [22905200](https://pubmed.ncbi.nlm.nih.gov/22905200/)
14. S. H. Duncan *et al.*, Human colonic microbiota associated with diet, obesity and weight loss. *Int. J. Obes. (London)* **32**, 1720–1724 (2008). doi: [10.1038/ijo.2008.155](https://doi.org/10.1038/ijo.2008.155); pmid: [18779823](https://pubmed.ncbi.nlm.nih.gov/18779823/)
15. A. Schwierz *et al.*, Microbiota and SCFA in lean and overweight healthy subjects. *Obesity (Silver Spring)* **18**, 190–195 (2010). doi: [10.1038/oby.2009.167](https://doi.org/10.1038/oby.2009.167); pmid: [19498350](https://pubmed.ncbi.nlm.nih.gov/19498350/)
16. A. Santacruz *et al.*, Gut microbiota composition is associated with body weight, weight gain and biochemical parameters in pregnant women. *Br. J. Nutr.* **104**, 83–92 (2010). doi: [10.1017/S0007114510000176](https://doi.org/10.1017/S0007114510000176); pmid: [20205964](https://pubmed.ncbi.nlm.nih.gov/20205964/)
17. R. Jumpertz *et al.*, Energy-balance studies reveal associations between gut microbes, caloric load, and nutrient absorption in humans. *Am. J. Clin. Nutr.* **94**, 58–65 (2011). doi: [10.3945/ajcn.110.010132](https://doi.org/10.3945/ajcn.110.010132); pmid: [21543530](https://pubmed.ncbi.nlm.nih.gov/21543530/)
18. A. Vrieze *et al.*, Transfer of intestinal microbiota from lean donors increases insulin sensitivity in individuals with metabolic syndrome. *Gastroenterology* **143**, 913, e7 (2012). doi: [10.1053/j.gastro.2012.06.031](https://doi.org/10.1053/j.gastro.2012.06.031); pmid: [22728514](https://pubmed.ncbi.nlm.nih.gov/22728514/)
19. P. Hakala, A. Rissanen, M. Koskenvuo, J. Kaprio, T. Rönnemaa, Environmental factors in the development of obesity in identical twins. *Int. J. Obes. Relat. Metab. Disord.* **23**, 746–753 (1999). doi: [10.1038/sj.ijo.0800923](https://doi.org/10.1038/sj.ijo.0800923); pmid: [10454109](https://pubmed.ncbi.nlm.nih.gov/10454109/)
20. A. Rissanen *et al.*, Acquired preference especially for dietary fat and obesity: A study of weight-discordant monozygotic twin pairs. *Int. J. Obes. Relat. Metab. Disord.* **26**, 973–977 (2002). pmid: [12080452](https://pubmed.ncbi.nlm.nih.gov/12080452/)
21. A. E. Duncan *et al.*, Genetic and environmental contributions to BMI in adolescent and young adult women. *Obesity (Silver Spring)* **17**, 1040–1043 (2009). doi: [10.1038/oby.2008.643](https://doi.org/10.1038/oby.2008.643); pmid: [19165159](https://pubmed.ncbi.nlm.nih.gov/19165159/)
22. M. Waldron, K. K. Bucholz, M. T. Lynskey, P. A. Madden, A. C. Heath, Alcoholism and timing of separation in parents: Findings in a midwestern birth cohort. *J. Stud. Alcohol Drugs* **74**, 337–348 (2013). pmid: [23384382](https://pubmed.ncbi.nlm.nih.gov/23384382/)
23. Materials and methods are available as supplementary material on Science Online.
24. E. Kristiansson, P. Hugenholtz, D. Dalevi, ShotgunFunctionalizeR: An R-package for functional comparison of metagenomes. *Bioinformatics* **25**, 2737–2738 (2009). doi: [10.1093/bioinformatics/btp508](https://doi.org/10.1093/bioinformatics/btp508); pmid: [19696045](https://pubmed.ncbi.nlm.nih.gov/19696045/)
25. C. B. Newgard *et al.*, A branched-chain amino acid-related metabolic signature that differentiates obese and lean humans and contributes to insulin resistance. *Cell Metab.* **9**, 311–326 (2009). doi: [10.1016/j.cmet.2009.02.002](https://doi.org/10.1016/j.cmet.2009.02.002); pmid: [19356713](https://pubmed.ncbi.nlm.nih.gov/19356713/)
26. B. D. Muegge *et al.*, Diet drives convergence in gut microbiome functions across mammalian phylogeny and within humans. *Science* **332**, 970–974 (2011). doi: [10.1126/science.1198719](https://doi.org/10.1126/science.1198719); pmid: [21596990](https://pubmed.ncbi.nlm.nih.gov/21596990/)
27. M. J. Keenan *et al.*, Effects of resistant starch, a non-digestible fermentable fiber, on reducing body fat. *Obesity (Silver Spring)* **14**, 1523–1534 (2006). doi: [10.1038/oby.2006.176](https://doi.org/10.1038/oby.2006.176); pmid: [17030963](https://pubmed.ncbi.nlm.nih.gov/17030963/)
28. J. Zhou *et al.*, Dietary resistant starch upregulates total GLP-1 and PYY in a sustained day-long manner through fermentation in rodents. *Am. J. Physiol. Endocrinol. Metab.* **295**, E1160–E1166 (2008). doi: [10.1152/ajpendo.90637.2008](https://doi.org/10.1152/ajpendo.90637.2008); pmid: [18796545](https://pubmed.ncbi.nlm.nih.gov/18796545/)
29. J. Zhou *et al.*, Failure to ferment dietary resistant starch in specific mouse models of obesity results in no body fat loss. *J. Agric. Food Chem.* **57**, 8844–8851 (2009). doi: [10.1021/jf901548e](https://doi.org/10.1021/jf901548e); pmid: [19739641](https://pubmed.ncbi.nlm.nih.gov/19739641/)
30. D. Knights *et al.*, Bayesian community-wide culture-independent microbial source tracking. *Nat. Methods* **8**, 761–763 (2011). doi: [10.1038/nmeth.1650](https://doi.org/10.1038/nmeth.1650); pmid: [21765408](https://pubmed.ncbi.nlm.nih.gov/21765408/)
31. J. P. Lessard, J. A. Fordyce, N. J. Gotelli, N. J. Sanders, Invasive ants alter the phylogenetic structure of ant communities. *Ecology* **90**, 2664–2669 (2009). doi: [10.1890/09-0503.1](https://doi.org/10.1890/09-0503.1); pmid: [19886475](https://pubmed.ncbi.nlm.nih.gov/19886475/)
32. M. T. Johnson, J. R. Stinchcombe, An emerging synthesis between community ecology and evolutionary biology. *Trends Ecol. Evol.* **22**, 250–257 (2007). doi: [10.1016/j.tree.2007.01.014](https://doi.org/10.1016/j.tree.2007.01.014); pmid: [17296244](https://pubmed.ncbi.nlm.nih.gov/17296244/)
33. C. O. Webb, N. C. Pitman, Phylogenetic balance and ecological evenness. *Syst. Biol.* **51**, 898–907 (2002). doi: [10.1080/10635150290102609](https://doi.org/10.1080/10635150290102609); pmid: [12554456](https://pubmed.ncbi.nlm.nih.gov/12554456/)
34. P. J. Turnbaugh *et al.*, An obesity-associated gut microbiome with increased capacity for energy harvest. *Nature* **444**, 1027–1031 (2006). doi: [10.1038/nature05414](https://doi.org/10.1038/nature05414); pmid: [17183312](https://pubmed.ncbi.nlm.nih.gov/17183312/)
35. P. Gauffin Cano, A. Santacruz, A. Moya, Y. Sanz, Bacteroides uniformis CECT 7771 ameliorates metabolic and immunological dysfunction in mice with high-fat-diet induced obesity. *PLoS ONE* **7**, e41079 (2012). doi: [10.1371/journal.pone.0041079](https://doi.org/10.1371/journal.pone.0041079); pmid: [22844426](https://pubmed.ncbi.nlm.nih.gov/22844426/)
36. S. H. Duncan *et al.*, Contribution of acetate to butyrate formation by human faecal bacteria. *Br. J. Nutr.* **91**, 915–923 (2004). doi: [10.1079/BJN20041150](https://doi.org/10.1079/BJN20041150); pmid: [15182395](https://pubmed.ncbi.nlm.nih.gov/15182395/)
37. M. A. Mahowald *et al.*, Characterizing a model human gut microbiota composed of members of its two dominant bacterial phyla. *Proc. Natl. Acad. Sci. U.S.A.* **106**, 5859–5864 (2009). doi: [10.1073/pnas.0901529106](https://doi.org/10.1073/pnas.0901529106); pmid: [19321416](https://pubmed.ncbi.nlm.nih.gov/19321416/)
38. Z. Gao *et al.*, Butyrate improves insulin sensitivity and increases energy expenditure in mice. *Diabetes* **58**, 1509–1517 (2009). doi: [10.2337/db08-1637](https://doi.org/10.2337/db08-1637); pmid: [19366864](https://pubmed.ncbi.nlm.nih.gov/19366864/)
39. H. V. Lin *et al.*, Butyrate and propionate protect against diet-induced obesity and regulate gut hormones via free fatty acid receptor 3-independent mechanisms. *PLoS ONE* **7**, e35240 (2012). doi: [10.1371/journal.pone.0035240](https://doi.org/10.1371/journal.pone.0035240); pmid: [22506074](https://pubmed.ncbi.nlm.nih.gov/22506074/)
40. H. Kuribayashi, M. Miyata, H. Yamakawa, K. Yoshinari, Y. Yamazoe, Enterobacteria-mediated deconjugation of taurocholic acid enhances ileal farnesoid X receptor signaling. *Eur. J. Pharmacol.* **697**, 132–138 (2012). doi: [10.1016/j.ejphar.2012.09.048](https://doi.org/10.1016/j.ejphar.2012.09.048); pmid: [23051670](https://pubmed.ncbi.nlm.nih.gov/23051670/)
41. J. R. Swann *et al.*, Systemic gut microbial modulation of bile acid metabolism in host tissue compartments. *Proc. Natl. Acad. Sci. U.S.A.* **108** (suppl. 1), 4523–4530 (2011). doi: [10.1073/pnas.1006734107](https://doi.org/10.1073/pnas.1006734107); pmid: [20837534](https://pubmed.ncbi.nlm.nih.gov/20837534/)
42. Y. Zhang *et al.*, Loss of FXR protects against diet-induced obesity and accelerates liver carcinogenesis in ob/ob mice. *Mol. Endocrinol.* **26**, 272–280 (2012). doi: [10.1210/me.2011-1157](https://doi.org/10.1210/me.2011-1157); pmid: [22261820](https://pubmed.ncbi.nlm.nih.gov/22261820/)
43. T. Inagaki *et al.*, Fibroblast growth factor 15 functions as an enterohepatic signal to regulate bile acid homeostasis. *Cell Metab.* **2**, 217–225 (2005). doi: [10.1016/j.cmet.2005.09.001](https://doi.org/10.1016/j.cmet.2005.09.001); pmid: [16213224](https://pubmed.ncbi.nlm.nih.gov/16213224/)
44. T. Li *et al.*, Transgenic expression of cholesterol 7 α -hydroxylase in the liver prevents high-fat diet-induced obesity and insulin resistance in mice. *Hepatology* **52**, 678–690 (2010). doi: [10.1002/hep.23721](https://doi.org/10.1002/hep.23721); pmid: [20623580](https://pubmed.ncbi.nlm.nih.gov/20623580/)
45. Y. Handelsman, Role of bile acid sequestrants in the treatment of type 2 diabetes. *Diabetes Care* **34** (suppl. 2), S244–S250 (2011). doi: [10.2337/dc11-s237](https://doi.org/10.2337/dc11-s237); pmid: [21525463](https://pubmed.ncbi.nlm.nih.gov/21525463/)
46. T. R. Koves *et al.*, Peroxisome proliferator-activated receptor-gamma co-activator 1alpha-mediated metabolic remodeling of skeletal myocytes mimics exercise training and reverses lipid-induced mitochondrial inefficiency. *J. Biol. Chem.* **280**, 33588–33598 (2005). doi: [10.1074/jbc.M507621200](https://doi.org/10.1074/jbc.M507621200); pmid: [16079133](https://pubmed.ncbi.nlm.nih.gov/16079133/)
47. T. R. Koves *et al.*, Mitochondrial overload and incomplete fatty acid oxidation contribute to skeletal muscle insulin resistance. *Cell Metab.* **7**, 45–56 (2008). doi: [10.1016/j.cmet.2007.10.013](https://doi.org/10.1016/j.cmet.2007.10.013); pmid: [18177724](https://pubmed.ncbi.nlm.nih.gov/18177724/)
48. D. M. Muoio *et al.*, Muscle-specific deletion of carnitine acetyltransferase compromises glucose tolerance and metabolic flexibility. *Cell Metab.* **15**, 764–777 (2012). doi: [10.1016/j.cmet.2012.04.005](https://doi.org/10.1016/j.cmet.2012.04.005); pmid: [22560225](https://pubmed.ncbi.nlm.nih.gov/22560225/)
49. J. S. Bakken *et al.*, Treating Clostridium difficile infection with fecal microbiota transplantation. *Clin. Gastroenterol. Hepatol.* **9**, 1044–1049 (2011). doi: [10.1016/j.cgh.2011.08.014](https://doi.org/10.1016/j.cgh.2011.08.014); pmid: [21871249](https://pubmed.ncbi.nlm.nih.gov/21871249/)

Acknowledgments: We thank D. O'Donnell, M. Karlsson, S. Wagoner, J. Guruge, R. Chamberland, M. Meier, and S. Deng for superb technical assistance; P. Ahern for help with FACS analysis; D. Hopper and S. Marion for their contributions to the recruitment of discordant twins from the MOAFTS cohort and for obtaining fecal samples for the present study; I. Halatchev for help in performing diet experiments; plus A. Reyes and N. McNulty for many helpful suggestions. S. Baumann and S. Fischer (Agilent Technologies, Santa Clara, CA) provided technical support for some of the metabolomics analyses including a gift of the Fiehn metabolite library. This work was supported in part by grants from the NIH (DK078669, DK70977, P30-AG028716, and DK58398), the Crohn's and Colitis Foundation of America, plus Kraft Foods and Mondelez International. Bacterial 16S rRNA pyrosequencing reads have been deposited in the European Bioinformatics Institute under accession numbers ERP003513 and ERP003512, as have shotgun pyrosequencing data sets from cecal microbial community DNA (ERP003514), microbial community RNA-Seq data sets (ERP003551), and draft genome data sets from cultured bacterial isolates (PRJEB3728–PRJEB3780). RNA-seq data sets have also been deposited in Gene Expression Omnibus (GEO) under accession number GSE48861. Author contributions: V.K.R. and J.I.G. designed the mouse experiments; A.C.H., A.E.D., and J.I.G. designed and implemented the clinical data collection; N.W.G., J.I.G., D.K.H., B.J.L., and M.C.M. designed the NHANES-based mouse diets; V.K.R., J.J.F., J.C., M.J.M., J.R.B., K.F., and O.I. generated the data; V.K.R., J.J.F., F.R., J.C., J.C.C., W.V.T., L.K.U., W.A.W., A.L.K., R.K., A.E.D., A.C.H., B.H., V.L., M.J.M., J.R.B., C.B.N., and J.I.G. analyzed the data; and V.K.R. and J.I.G. wrote the paper.

Supplementary Materials

www.sciencemag.org/cgi/content/341/6150/1241214/suppl/DC1

Materials and Methods
Supplementary Text
Figs. S1 to S17
Tables S1 to S17
References (50–76)

30 May 2013; accepted 12 July 2013
10.1126/science.1241214